Title
Hovering performance of Anna's hummingbirds (Calypte anna) in ground effect

Journal
Journal of The Royal Society Interface, 11(98)

ISSN
1742-5689

Authors
Kim, Erica J
Wolf, Marta
Ortega-Jimenez, Victor Manuel
et al.

Publication Date
2014-09-06

DOI
10.1098/rsif.2014.0505

Peer reviewed

JOURNAL OF THE ROYAL SOCIETY Interface

rsif.royalsocietypublishing.org

Research

Cite this article: Kim EJ, Wolf M, Ortega-Jimenez VM, Cheng SH, Dudley R. 2014 Hovering performance of Anna's hummingbirds (*Calypte anna*) in ground effect. *J. R. Soc. Interface* **11**: 20140505.
http://dx.doi.org/10.1098/rsif.2014.0505

Received: 14 May 2014
Accepted: 9 June 2014

Subject Areas:
biomechanics, bioenergetics

Keywords:
ground effect, hovering, induced velocity, metabolic power, vortex wake

Author for correspondence:
Victor Manuel Ortega-Jimenez
e-mail: vortega@berkeley.edu

Electronic supplementary material is available at http://dx.doi.org/10.1098/rsif.2014.0505 or via http://rsif.royalsocietypublishing.org.

Royal Society Publishing

Hovering performance of Anna's hummingbirds (*Calypte anna*) in ground effect

Erica J. Kim[1], Marta Wolf[4], Victor Manuel Ortega-Jimenez[2], Stanley H. Cheng[3] and Robert Dudley[2,5]

[1]Biophysics Graduate Program, [2]Department of Integrative Biology, and [3]Department of Molecular Cell Biology, University of California, Berkeley, CA 94720-3200, USA
[4]Department of Biology, Lund University, Lund, Sweden
[5]Smithsonian Tropical Research Institute, Balboa, Republic of Panama

Aerodynamic performance and energetic savings for flight in ground effect are theoretically maximized during hovering, but have never been directly measured for flying animals. We evaluated flight kinematics, metabolic rates and induced flow velocities for Anna's hummingbirds hovering at heights (relative to wing length $R = 5.5$ cm) of $0.7R$, $0.9R$, $1.1R$, $1.7R$, $2.2R$ and $8R$ above a solid surface. Flight at heights less than or equal to $1.1R$ resulted in significant reductions in the body angle, tail angle, anatomical stroke plane angle, wake-induced velocity, and mechanical and metabolic power expenditures when compared with flight at the control height of $8R$. By contrast, stroke plane angle relative to horizontal, wingbeat amplitude and wingbeat frequency were unexpectedly independent of height from ground. Qualitative smoke visualizations suggest that each wing generates a vortex ring during both down- and upstroke. These rings expand upon reaching the ground and present a complex turbulent interaction below the bird's body. Nonetheless, hovering near surfaces results in substantial energetic benefits for hummingbirds, and by inference for all volant taxa that either feed at flowers or otherwise fly close to plant or other surfaces.

1. Introduction

Flying near the ground or near any other boundary can potentially influence aerodynamic performance [1–4]. In this so-called ground effect, interaction between the vortex wake generated in flight and the lower boundary reduces the mean induced velocity, and thus both the induced and total powers required to hover [5]. Lighthill [6] pointed out that reduction of the induced velocity can be viewed as an interaction between the vortex wake generated by the wings and an opposing vortex structure actuated by the ground via a mirroring effect. Whereas the aerodynamic advantages of forward locomotion in ground effect have been modelled for birds [7–9], little brown bats [10] and flying fish [11] (see also [12–14]), the actual mechanical as well as metabolic consequences of such flight have yet to be systematically characterized. These advantages would be expected to be maximal for hovering, based on the associated power savings experimentally found for helicopters flying close to the ground [1,2,5].

In comparison with rotor aircraft, relatively little is known about the vortex wake for animals hovering in ground effect. Flow visualization of the helicopter wake in ground effect indicates a reduction in the axial descent speed of the tip vortices, along with wake compression and lateral expansion of these vortices as they approach the ground [15] (for geometrical details, see fig. 5.35 of [1]). Computational analyses for simple insect models and simulations of two-dimensional aerofoils hovering in ground effect suggest similar vortex structures [16,17]. However, given the three-dimensional complexities of flapping wings, it is possible that the associated vortex wakes generated during ground effect for animals differ from those predicted theoretically. Furthermore, if and how animals

change their kinematics in response to ground proximity is not clear, owing to the somewhat inconsistent results found within the literature. For example, hovering mandarin fish increase their fin stroke amplitude while in ground effect [12]; by contrast, plaice in forward swimming decrease tailbeat amplitude and frequency, whereas swimming cod do not make any changes at all [13]. For volant taxa, the effects of ground distance on flight kinematics and power expenditure are particularly unresolved.

Although hummingbirds rarely hover near the ground, they often feed from flowers surrounded by other vegetational surfaces; this can potentially induce a ground effect if the air transmissivity of the foliage matrix is low. More importantly, hummingbirds can serve to illustrate general biomechanical patterns that pertain to other nectarivorous taxa (e.g. many insects, bats and other nectarivorous birds) which commonly hover above leaves and floral structures, as well as predatory hymenopterans and much smaller parasitoids which fly near the ground or over larvae either on or within leaves. Because hummingbirds represent a particularly convenient model system with which to assess the mechanics of flight in ground effect, given the ease with which they hover in laboratory contexts as well as the feasibility of measuring their metabolic rates during various aerodynamic tasks [18–20], we seek here to characterize wing and body kinematics, mechanical power expenditures, metabolic rates and wake-induced velocities for Anna's hummingbird (*Calypte anna*) hovering both in ground effect and out of ground effect. We predict that hummingbirds hovering in ground effect will decrease their induced velocity without any concurrent changes in wing kinematics, in comparison with control flight.

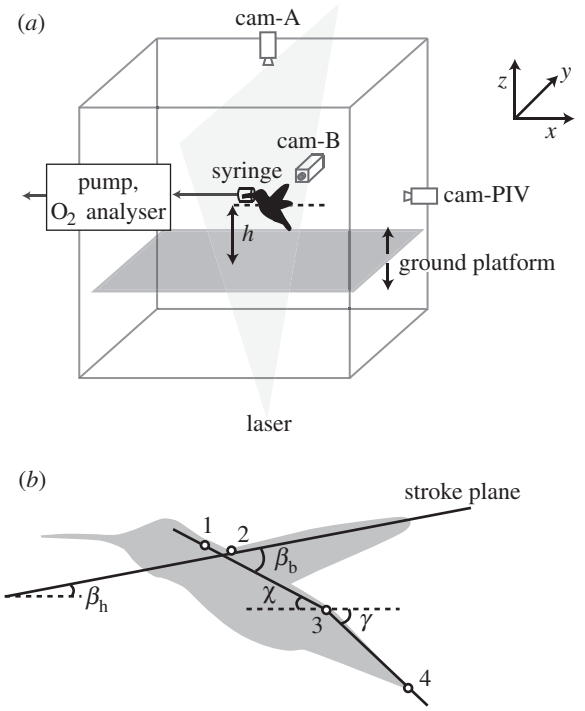

Figure 1. (*a*) Experimental configuration for kinematic, metabolic and PIV measurements (note that these measurements were made separately on any given bird, not simultaneously). The global coordinate system as well as positions of the syringe, moving platform, high-speed cameras ('cam-A' and 'cam-B'), pull-through respirometry system and PIV system (laser sheet and 'cam-PIV') are labelled. (*b*) Landmarks for the bird's neck (1), right shoulder (2), rump (3) and tail tip (4); angles for the stroke plane and anatomical stroke plane (β_h and β_b, respectively), and body and tail angle (χ and γ, respectively) are also indicated. A positive tail angle denotes that the vector between rump and tail tip point is oriented below the (*x*,*y*) plane, whereas a negative tail angle denotes that the vector is oriented above this plane.

2. Material and methods

Four male Anna's hummingbirds (mean body mass $m \pm 1$ s.d.: 4.7 ± 0.2 g (range of 4.5–5.0 g)) were trained to hover-feed within a Plexiglas cube ($90 \times 90 \times 90$ cm). A syringe filled with a 20% solution of Nektar-Plus (Nekton GmbH, Pforzheim, Germany) and tipped with a respirometry mask was placed within the cube's centre (figure 1*a*). A transparent Plexiglas platform (61×77 cm), which served as a ground surface, was positioned at variable distances beneath the syringe. The ground height h, defined here as the perpendicular distance between this platform and the centre of the respirometry mask, was altered by moving the platform up or down along the vertical z-axis. Six values of h were used in experiments, corresponding to heights of $0.7R$ (4 cm), $0.9R$ (5 cm), $1.1R$ (6 cm), $1.7R$ (9 cm), $2.2R$ (12 cm) and $8R$ (43 cm), where R was the average wing length (5.45 ± 0.05 cm) for the four experimental hummingbirds. Treatment orders were selected randomly to minimize any order bias. Heights lower than $0.7R$ were not tested, as physical contact between birds and the platform (via either the feet or the tail) frequently occurred. The maximum ground distance of $8R$ served as the control treatment. As distances between the syringe and the chamber's walls were typically 7–8 wing lengths in all cases, aerodynamic effects of sidewalls were assumed to be insignificant, according to a theoretical analysis of the recirculation effects for animal fliers within a confined volume (see fig. 4 in [5]).

2.1. Flight kinematics and energetics

At each of the aforementioned height treatments, each bird was filmed three times (mean video duration was five wingbeats, corresponding to about 0.11 s of film) during the course of an experimental trial. We used two synchronized high-speed video cameras (X-PRI, AOS Technologies AG, Baden Daettwil, Switzerland), recording at 1000 frames s^{-1} (800×600 pixels), positioned above and laterally to the hovering bird (figure 1*a*). Three-dimensional calibrations and digitization were carried out in ProAnalyst (Xcitex Inc.). For each video frame, marked coordinates of the right wing tip, right shoulder, rump, centre tail tip and neck (figure 1*b*) were digitized and imported into Matlab (v. 7.8.0.347). We calculated the stroke plane by finding the best-fit plane, based on principal component analysis, for positions of the wingtip and shoulder points throughout the course of each video. We subsequently calculated body angle χ, tail angle γ, horizontal stroke plane angle β_h, anatomical stroke plane angle β_a (see [21]), stroke amplitude Φ and wingbeat frequency n with custom Matlab code, where, using the coordinate system as depicted in figure 1*a*, we defined χ, γ and β_h as the acute angles between the XY-plane and the stroke plane, the vector from neck to rump and the vector from rump to tail tip, respectively, and β_a as the sum of β_h and χ. We estimated the flapping frequency n (i.e. angular frequency$/2\pi$) from a sinusoidal curve fit using the bird's wingtip z-coordinate positions as a function of time. Wingbeat amplitude Φ was estimated by measuring the average angle formed by the wingtip at the start of each downstroke, the shoulder and the wingtip at the end of the downstroke. Horizontal and anatomical stroke plane angles were calculated for only three birds; because of a low shutter speed used in the lateral video recordings for one individual, lateral tracking of the wingtip was difficult and thus omitted. Kinematic variables for each bird were averaged over the three separate video sequences, yielding a total of 60 wing beats per

treatment (four birds × three video sequences per bird × five wingbeats per video sequence) for estimates of χ, γ, Φ and n, and a total of 45 wing beats per treatment (three birds × three video sequences per bird × five wingbeats per video sequence) for estimates of β_a and β_h.

The metabolic power input (P_{met}) during hover-feeding was estimated from measurements of the rate of oxygen consumption via the use of a pull-through mask respirometry system [22]. As the birds hovered and fed, expired gas was first drawn into the respirometry mask (fashioned from the tip of a 10 ml plastic syringe) at a rate of 1200 ml O_2 min^{-1}, water-scrubbed with Drierite (W. A. Hammond Drierite Co. Ltd), and then passed into an O_2 analyser equipped with a flow meter (FOXBOX-C field gas analysis system, Sable Systems International). A photoresistor-LED circuit, modelled after that of Bartholomew & Lighton [22], indicated the presence of the bird's head within the mask, thereby enabling accurate measurements of feeding duration. As all of the hummingbirds fed for relatively short durations (mean of 4.98 s), oxygen consumption rates infrequently reached steady-state values. We therefore estimated the oxygen consumption rate by dividing the total volume of depleted O_2 by the total summed feeding time, using only those feeding bouts with durations greater than 2 s in our analysis [22,23]. Because hummingbirds had unlimited access to the sugar-dense Nektar-Plus solution, we used a respiratory quotient of one [24] and an energy conversion factor of 21.1 J ml^{-1} O_2 [25] for subsequent metabolic calculations. A mean of 12 metabolic measurements were made for each bird per treatment over a period of 3 days.

Total mechanical power output, assuming perfect elastic storage, P_{mech} [26], was calculated for three birds as the sum of the profile power P_{pro} and the induced power P_{ind}, where P_{ind} and P_{pro} correspond to the rates of energy expenditure required to generate vertical force, and to overcome both form and skin friction drag of the wings, respectively. We estimated P_{ind} as the product of the weight and the induced velocity V_{ind}, where V_{ind} was explicitly measured, as described below. We estimated P_{pro} following Ellington [26], but used the values of induced velocity that we directly measured for calculations. We additionally used a profile drag coefficient of 0.139 based on the drag measurements made on a revolving hummingbird wing at Re of 5000 and angle of attack of 15° (see fig. 5 from [27]), rather than estimating the coefficient based on wing mean Reynolds number [26]. This approach does not capture the variation in profile drag deriving from changes in angles of incidence associated with variable flow fields, but is intended here as a first approximation for comparison with induced power estimates. Muscle efficiency η was estimated as the ratio of mechanical power output to metabolic power input, with the added assumption that only 90% of the metabolic power was expended by the flight muscles [28].

2.2. Vortex wake visualization and quantification

Smoke visualization technique was used to obtain qualitative details of the vortex wake for one hummingbird. A separate wire cube structure (30 × 30 × 30 cm) with a Plexiglas floor was covered at the top and all sides with mesh fabric. A syringe containing Nektar-Plus was placed within the cube, either at 0.9R (5 cm) above the floor to resemble in ground effect conditions, or at 2.2R (12 cm) above the floor to simulate out of ground effect conditions. Owing to the porous nature of the mesh walls and top, we assumed that the only aerodynamic effect of the cube on the hummingbird's wake came from the solid ground surface. To visualize the airflow, a water-based, non-toxic smoke (American DJ ecowater-based fog juice) generated by a smoke machine (Eliminator E119 FOGIT) was forced into the cube from above. To reduce the initially high flow rate (approx. 100 m^3 min^{-1}), four layers of mesh were used as a filter to laminarize flow and to reduce the rate by one to two orders of magnitude. A continuous 200 mW laser (532 nm Spyder II GX, Wicked Lasers) with a quartz cylindrical optic illuminated the fog along the dorsal plane of the hummingbird's wake, whereas a video camera (Sony HDR-UX1, 1440 × 1080) oriented orthogonally to the laser sheet recorded the flow field at 120 frames s^{-1}. Video sequences of the hummingbird hover-feeding were then de-interlaced using the program Avidemux, yielding an effective filming speed of 240 frames s^{-1}.

For three hummingbirds, particle imaging velocimetry (PIV) was used to quantitatively characterize their vortex wakes at each height treatment. Birds were first trained for several days to hover-feed in the aforementioned Plexiglas flight cube in a low-light environment. For PIV experiments, the cube's interior was seeded approximately 20 s prior to filming with a cloud of volatilized olive oil droplets (approx. 1 µm in diameter) generated by a LaVision vaporizer at a rate of approximately 1.4×10^{10} particles s^{-1}. The vaporizer was positioned at the open side door to the flight cube; this door was closed following seeding to minimize any subsequently induced flows which in any event would be insignificant relative to the convection generated by hummingbird wing motions. We illuminated these volatilized oil droplets using a 2 mm thick laser sheet in the transverse plane just behind the trailing edge of the wing (approx. 0–2 cm from the wingroot), using a double pulsed 50 mJ Nd:YAG laser (532 nm New Wave Research SoloPIV) running at a pulse repetition rate of 15 Hz. An Image ProX CCD camera (1600 × 1200 pixels), synchronized with and positioned perpendicular to the laser sheet, was used to capture sequences of 24 pair-wise images ($dt = 100$ µs) over an approximately 15 × 20 cm^2 area. The camera was equipped with a 52 mm f/1.8D Nikon lens with the aperture set at 1.8. We used LaVision Davis software (v. 7.2.1.76) with multi-pass correlation (128 × 128 and 32 × 32, 50% overlap) to process images and to derive particle displacements. Images were then post-processed using a peak ratio deletion ($Q < 1.3$), a median vector filter that removed vectors larger than twice the neighbouring r.m.s. velocity, and a single 3 × 3 smoothing average.

From all of the recorded PIV sequences, 100 images were chosen for each bird at each height treatment. In order to consistently obtain images in which the vortex wake was unmistakably identifiable across all treatments, we analysed the wake only during the mid-downstroke phase of the wingbeat. To estimate the potential error introduced by this selection bias, we also made 25 measurements of the far wake velocity w for an entire wingbeat, for three birds at the control height (electronic supplementary material, table S1). We measured w in the region between the wing edge and 4 cm beneath each of the wings, at a position between the wingtip and root vortices. As there was no significant difference between PIV measurements for the left and right wings' wakes, estimates of wake velocities were averaged for the two sides. The induced velocity was then calculated as $V_{ind} = 0.5\,w$ in accordance with momentum theory [1,2].

2.3. Statistical analysis

Repeated-measures ANOVA was performed for each of the dependent variables χ, γ, β_h, β_a, Φ, n, P_{mech}, P_{met}, V_{ind} and η, using distance from ground as the independent variable (i.e. a within-subjects factor). Tukey's *post hoc* tests were then carried out to determine statistically significant differences among treatments. All parameters fulfilled both normality conditions (Shapiro–Wilk test, $p > 0.05$ for all cases) and equality of variance (Bartlett's tests, $p > 0.05$ for all cases). A Huynh–Feldt correction was applied to variables in which sphericity was violated (i.e. $p < 0.05$ for Mauchly's test). We also used a Kruskal–Wallis test to determine if our in ground effect/out of ground effect ratios for mechanical and metabolic power expenditure were comparable to values predicted by two theoretical models for helicopters (Cheeseman &

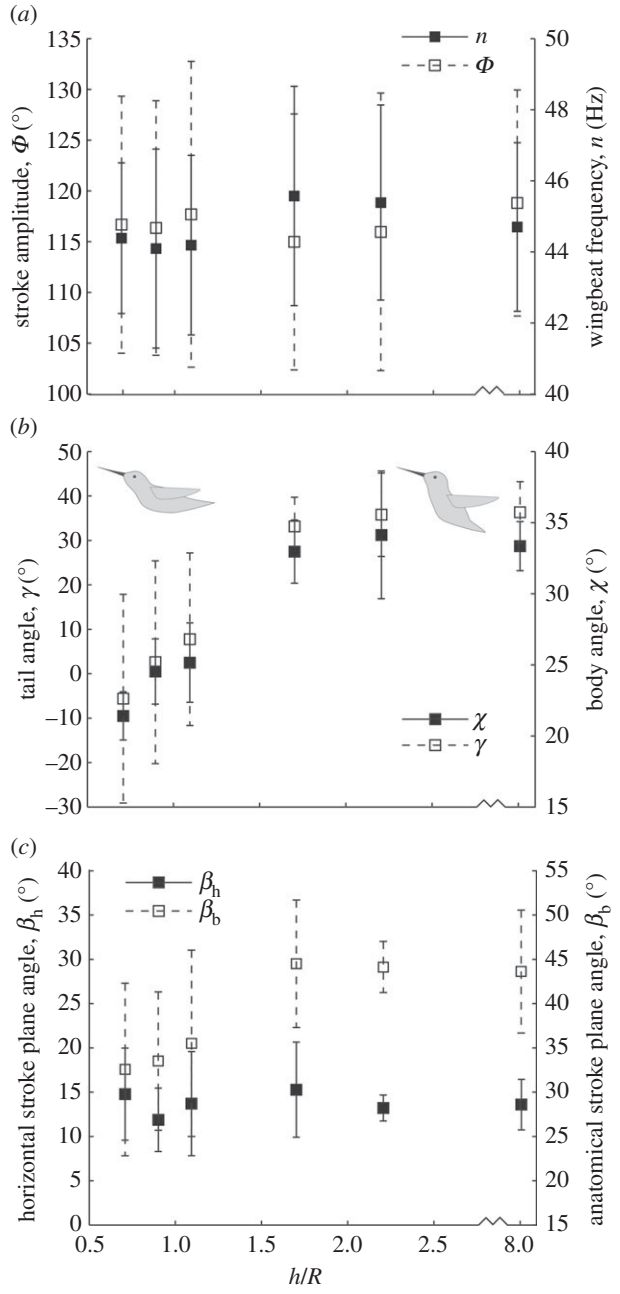

Figure 2. (*a*) Stroke amplitude Φ and wingbeat frequency n; (*b*) tail angle γ and body angle χ; (*c*) horizontal stroke plane angle β_h and anatomical stroke plane angle β_b, all as functions of the normalized ground distance (h/R). Data are presented as mean values $\pm$ 1 s.d., with $N = 4$ for all variables except β_h and β_b, for which $N = 3$.

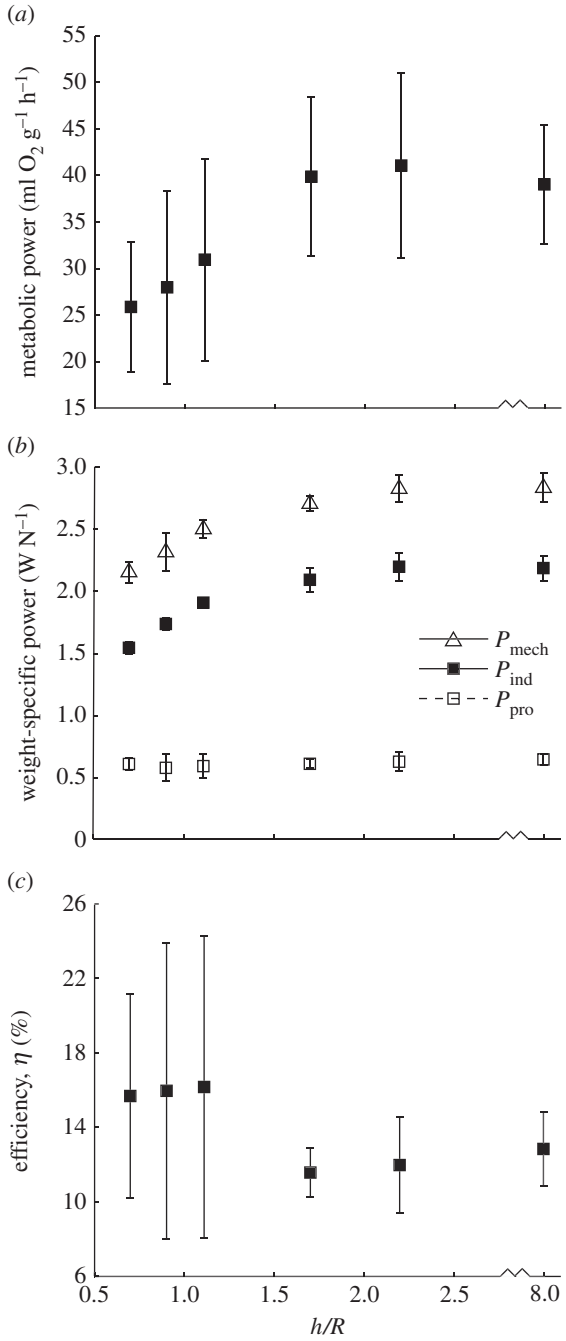

Figure 3. (*a*) Metabolic rate, (*b*) body-weight specific profile power, induced power, and total mechanical power and (*c*) efficiency, all as functions of the normalized ground distance (h/R). Data are presented as mean values $\pm$ 1 s.d., with $N = 4$ for metabolic rates and $N = 3$ for all other data.

Bennett's model, and Hayden's model; see [1]). All statistical tests were carried out in R v. 2.10.1 (R Development Core Team).

3. Results

Repeated-measures ANOVAs indicated significant differences with ground height in body angle ($F_{14.5}$, d.f. = 5,15, $p = 2.3 \times 10^{-4}$; figure 2*b*), tail angle ($F_{14.9}$, d.f. = 5,15, $p = 1.6 \times 10^{-3}$; figure 2*b* and electronic supplementary material, table S2), anatomical stroke plane angle ($F_{11.1}$, d.f. = 5,10, $p = 0.012$; figure 2*c*), metabolic power ($F_{14.3}$, d.f. = 5,15, $p = 5.5 \times 10^{-4}$; figure 3*a*), induced velocity ($F_{48.5}$, d.f. = 5,10, $p = 3 \times 10^{-3}$) and mechanical power ($F_{37.9}$, d.f. = 5,10, $p = 8.7 \times 10^{-6}$; figure 3*b*). By contrast, no significant variation with ground height was found for the horizontal stroke plane angle ($F_{2.7}$, d.f. = 5,15, $p = 0.2$; figure 2*c*), wingbeat frequency ($F_{1.5}$, d.f. = 5,15, $p = 0.8$; figure 2*a*) and stroke amplitude ($F_{0.4}$, d.f. = 5,15, $p = 0.3$; figure 2*a*). *Post hoc* tests indicated that hummingbirds hovering at ground distances equal to $0.7R$, $0.9R$ and $1.1R$ (but not at $1.7R$ or $2.1R$) exhibited significantly lower values of χ, β, P_{met}, V_{ind} and P_{mech} than at the control height of $8R$ (table 1).

Maximal reductions in P_{met}, V_{ind}, and P_{mech} owing to the ground effect were 34%, 29% and 24%, respectively. Whereas there was a 5% increase in flight muscle efficiency at $h/R = 0.7$, 0.9, and 1.1 compared with the control height, this difference was not statistically significant ($F_{1.39}$, d.f. = 5,10, $p = 0.36$; figure 3*c*). We found that w measured during mid-downstroke gives values 15% higher than when measured for the entire stroke (two-way ANOVA; $F_{167.6}$, d.f. = 1,149,

Table 1. Mean values ± 1 s.d. of kinematic variables ($N = 4$ for all variables except β_h and β_b, for which $N = 3$), metabolic power ($N = 4$), wake-induced velocity ($N = 3$), mechanical power ($N = 3$) and efficiency ($N = 3$) at different values of normalized ground height (h/R).

h/R	χ (°)	γ (°)	β_h (°)	β_b (°)	Φ (°)	n (Hz)	P_{met} (ml O_2 g^{-1} h^{-1})	V_{ind} (m s^{-1})	P_{mech} (W N^{-1})	η (%)
0.7	21.4 ± 1.7	−5.6 ± 23.5	14.8 ± 5.2	32.5 ± 9.7	115.3 ± 7.4	44.8 ± 3.6	25.9 ± 7.0	1.5 ± 0.0	2.2 ± 0.1	15.7 ± 5.5
0.9	24.5 ± 2.3	2.6 ± 22.8	11.9 ± 3.6	33.4 ± 7.8	114.3 ± 9.8	44.7 ± 3.6	28.0 ± 10.4	1.7 ± 0.0	2.3 ± 0.2	15.9 ± 7.8
1.1	25.1 ± 2.8	7.8 ± 19.4	13.7 ± 5.9	35.4 ± 10.5	114.7 ± 8.8	45.1 ± 4.3	30.9 ± 10.9	1.9 ± 0.0	2.5 ± 0.1	16.2 ± 8.1
1.7	33.0 ± 2.2	33.1 ± 6.6	15.3 ± 5.4	44.4 ± 7.2	119.5 ± 10.8	44.3 ± 3.6	39.9 ± 8.5	2.1 ± 0.1	2.7 ± 0.1	11.6 ± 1.3
2.2	34.1 ± 4.5	35.8 ± 9.4	13.2 ± 1.5	44.0 ± 2.9	118.9 ± 9.6	44.6 ± 3.9	41.1 ± 10.0	2.2 ± 0.1	2.8 ± 0.1	12.0 ± 2.6
8.0	33.3 ± 1.7	36.3 ± 6.9	13.6 ± 2.9	43.5 ± 6.9	116.4 ± 8.3	45.4 ± 3.2	39.0 ± 6.4	2.2 ± 0.1	2.8 ± 0.1	12.8 ± 2.0

$p = 2 \times 10^{-16}$). By contrast, we found no significant differences among birds (two-way ANOVA; $F_{0.86}$, d.f. = 2,148, $p = 0.4$). We also found no significant differences between in ground effect/out of ground effect ratios for either mechanical or metabolic power and the predicted values derived from Chesseman–Bennett and Hayden's models (Kruskal–Wallis test, $\chi^2 = 1.1$, d.f. = 4, $p = 0.89$).

Both PIV results and smoke visualization of the bird's wake revealed vortex rings derived from each wing during both up- and downstroke. However, visual clarity of these vortex ring pairs was substantially better defined during the downstroke (figure 4). Qualitative observations revealed that, during hovering at $h = 2.2R$, the two vortex rings descended axially and eventually dissipated, with relatively minimal mutual interaction. During hovering at $h = 0.9R$, however, the rings shed from each wing interacted both with the ground surface and with one another. Although this interaction resulted in a highly complicated three-dimensional flow pattern, certain repeated phenomena were observed (figure 5). Upon impacting the ground, each vortex was stretched laterally and thus asymmetrically. The innermost sides of the paired rings collided with one another beneath the hummingbird's body, and rolled upwards in a turbulent flow maintained by subsequent pairs of shed vortex rings. The outer edges of the paired rings, by contrast, appeared to travel along the ground away from the bird.

4. Discussion

Hummingbirds experienced substantial reductions in both mechanical and metabolic power expenditure (by up to 24% and 34%, respectively) when hovering at heights less than $1.7R$ above the ground (figure 3*b*). The magnitude of these reductions is comparable, at equivalent relative ground heights, to previously published theoretical estimates for helicopters hovering in ground effect [1,2,29,30] (figure 6). Reductions in the mechanical power found for hummingbirds were also broadly similar to those (15–25%) calculated for mandarin fish hovering in water at comparable fin lengths above a surface [12]. Whereas these fish concurrently decreased fin stroke frequency and increased fin stroke amplitude while in ground effect [12], there were no significant changes in n and Φ for the hummingbirds in this study. Experimental evidence from a flapping robotic wing suggests that beetles during take-off increase lift production by up to 18% at a ground height of $0.5R$ [31]. Moreover, a three-dimensional computational fluid dynamics simulation of a fruit fly hovering at a height of $0.8R$ shows increases in vertical forces by up to approximately 9% compared with those generated out of ground effect [32]. For hummingbirds flying in ground effect, rollup of the innermost edges of the generated vortex rings created a region of relatively continuous upwash directly beneath the bird's body; this flow, termed the 'fountain effect' [32], could underlie the observed postural changes observed in hummingbirds and may be generally relevant to in ground effect flight.

For helicopters hovering in ground effect with constant vertical force (as opposed to hovering with constant power), reduction in the downwards induced velocity yields an effective decrease in aerodynamic angles of attack [1], reducing blade pressure and total power expenditure. Qualitatively, we observed no substantial changes in the geometrical angle of

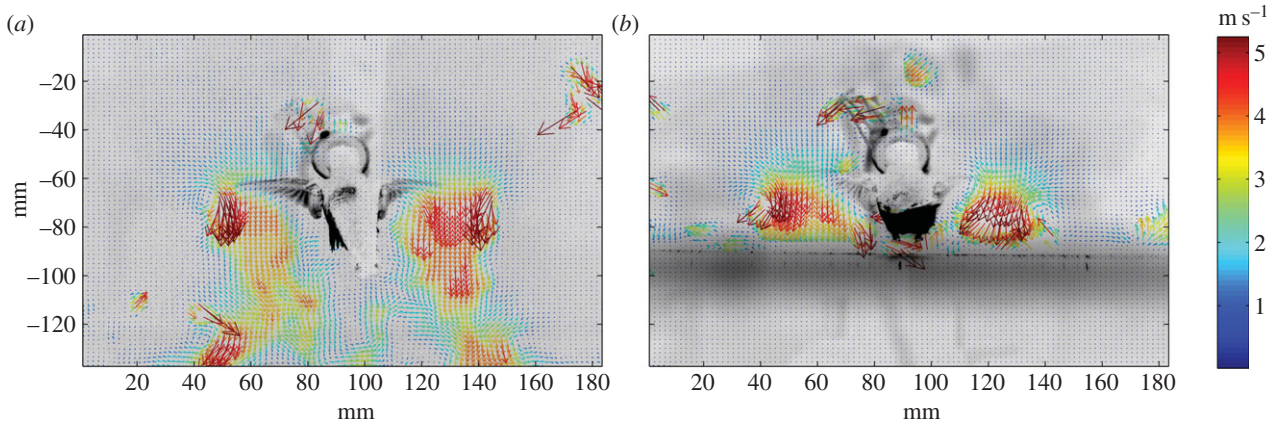

Figure 4. PIV vector fields for a hummingbird hovering in ground effect at 4 cm (*a*) and out of ground effect at 9 cm (*b*) from the ground. Note that the large clusters of high-velocity vectors are due to particles misidentified when the turbulence is high, when the feeder interferes with the view of particles or the particles move out of frame.

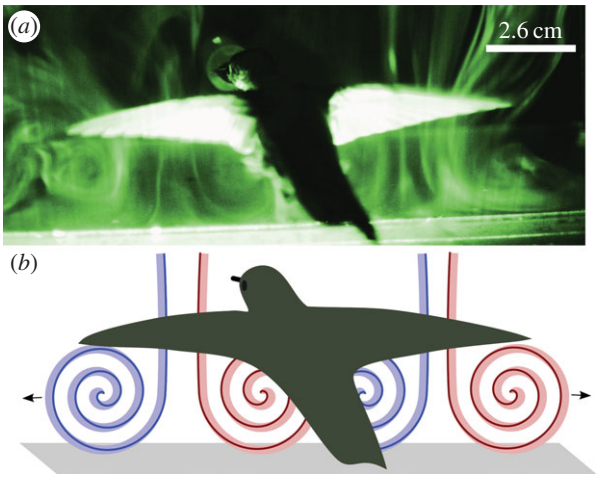

Figure 5. Smoke visualization of the hummingbird's hovering wake in ground effect at 5 cm: (*a*) raw video frame and (*b*) stylized reconstruction highlighting primary wake structures. Black arrows indicate vortex translation, whereas blue and red lines indicate clockwise and anticlockwise motions of the vortex, respectively.

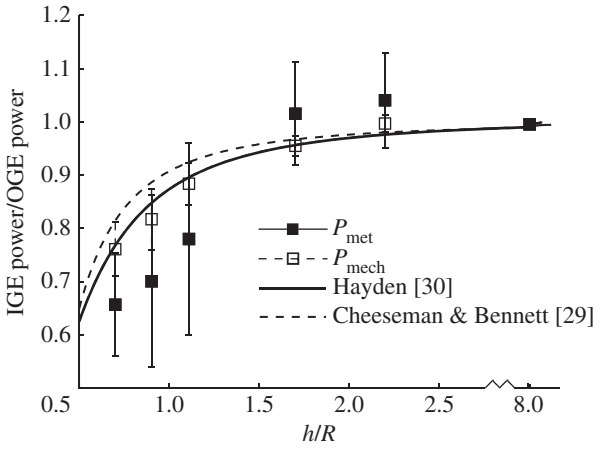

Figure 6. Comparison of average weight-normalized mechanical power estimates for Anna's hummingbirds with theoretical estimates derived from two helicopter models for hovering in ground effect (IGE) and out of ground effect (OGE) ([28,29]; as cited in [1,2]), with vertical thrust assumed to be constant. Error bars correspond to $\pm$ 1 s.d. ($N = 3$).

attack for hummingbirds flying in ground effect and out of ground effect (electronic supplementary material, video S2), although small changes may nonetheless ensue and, given typical nonlinearity in the lift polar for animal wings at low angles of attack, result in significant changes in profile drag and associated power. However, trends in total power expenditure are largely driven by the relatively large magnitude of induced power with respect to the profile power (figure 3*b*). Profile power (assuming a constant drag coefficient of 0.139) represents only 20–25% of total power, but if the profile drag out of ground effect is increased, via an assumed increase in mean angle of attack (because of a reduced induced velocity), it would decrease the correlation between mechanical and metabolic power (figure 3*a*,*b*). On the contrary, assuming a decreased profile drag in ground effect will reduce the modest estimates of profile power even further, and will only marginally change the aforementioned correlation as total power is driven primarily by the trend in induced power. Relevant unsteady drag data for hummingbird wings flapping at different angles of attack are in any event unavailable, but we consider the overall mechanical power trends derived here to be reliable, given the dominant role of the induced power component. Thus, we found full support for our initial predictions, based on helicopter theory, that the induced velocity decreases while the wing kinematics remain unchanged, with respect to ground height, for hovering hummingbirds.

In contrast to wingbeat kinematics, both body and tail angles changed significantly with ground height, with hummingbirds adopting a more horizontal body posture when hovering in ground effect compared with out of ground effect (figure 2*b*). Although all hummingbirds in this study decreased their tail angle in ground effect, the relative extent of such reduction varied considerably among individuals, resulting in large standard deviations in γ at $h/R \leq 1.1$ (figure 2*b*). Some individuals occasionally allowed either their tail or feet to touch the ground while hover-feeding at the lowest heights (such cases were excluded from the analyses presented here); other individuals, however, appeared to keenly avoid contacting the ground surface, exhibiting negative tail angles as large as $\gamma = -30^{\circ}$. Body angle changes mirrored those in tail angle, such that χ and γ changed concurrently. It is well known that aircraft in ground effect experience pitch instability, which is usually corrected by a highly elevated tail plane in order to shift the centre of pitch downstream while maintaining the aerodynamic centre of height upstream (for details, see [33]). Altshuler *et al.* [34] proposed that hummingbirds use their tails to deflect the flow created by the wings in order to maintain pitch stability

(see also [35] for use of tail in pitch recovery by a passerine bird). Changes in body angle might thus necessitate a concomitant change in tail angle in order to effect stability in pitch. Equivalently, of course, an externally imposed change in tail angle would require alteration of body angle.

Alternatively, a change in body posture could reflect the obvious differences between in ground effect and out of ground effect hovering in the overall surrounding flow. For a rotorcraft hovering in ground effect, the wake first descends axially, impacts the ground surface and then subsequently undergoes lateral expansion [36]. Smoke visualizations of rotors hovering in ground effect also reveal a region of stagnant fluid in the centre of the wake [36,37]. We observed a similar effect in hummingbirds, except that the wings shed pairs of vortices (figure 5*a*), rather than the single helical wake of rotors or the hypothesized single vortex previously described for hovering hummingbirds [38]. Recent PIV studies have shown that the near wake generated by a hummingbird during hovering is composed of two distinct vortex rings [39,40]. The rollup of the innermost edges of the rings created a region of relatively continuous upwash directly beneath the bird's body (see also [32]), which was qualitatively observed but not quantified in this experiment. This flow, termed the 'fountain effect' [32], could underlie the observed postural changes observed in hummingbirds and may be generally relevant to in ground effect flight. As the model used here for estimating mechanical power did not take into account this potentially beneficial phenomenon, P_{mech} could be overestimated, resulting in the higher (albeit statistically insignificant) muscle efficiency values found for birds hovering in ground effect relative to out of ground effect (figure 3*c*).

Additionally, we found a high interindividual variance in efficiency estimates for flight in ground effect, driven mostly by mass-specific rates of oxygen consumption for one bird (no. 2) that were approximately 50% less than those consumed by the other two birds in those treatments (see the electronic supplementary material, table S2). Mass-specific metabolic rates for the same bird flying out of ground effect were also much lower than other sampled birds. For flight in ground effect, this bird exhibited both stroke plane and tail angles substantially lower than those of the other two birds as well, which suggest that specific postural and kinematic changes may potentially increase savings for in ground effect hovering. However, a much increased sample size would be necessary to test this hypothesis.

Whereas Anna's hummingbirds tend to avoid flowers close to the ground in order to avoid terrestrial predators [41], observations of other hummingbird taxa suggest occasional flight near surfaces. For example, little hermits (*Phaethornis longuemareus*) forage for spider and insect prey in close proximity to the ground, and red-footed plumeleteers (*Chalybura urochrysia*) take arthropods from the upper surfaces of leaves [42]. We have also seen hovering hummingbirds picking insects directly off a dirt road in the Yucatan Peninsula (V.M.O.J. 2002, personal observation). Although it is unknown whether hummingbirds purposefully exploit the ground effect when either foraging for arthropods or during other activities, flight near vegetational surfaces at varied orientations is commonplace during nectar-feeding by other taxa. Energetic advantages of flight near boundaries may thus yield a small, but significant reduction in overall foraging costs for many other species that fly near solid boundaries, including such insects as empidid flies, caddisflies, stoneflies, mayflies and some species of butterflies (e.g. species within the *Cithaerias*, *Haetera* and *Pierella* genera) [43].

In conclusion, we found that hummingbirds obtain substantial mechanical and metabolic energy savings (of up to 24% and 34%, respectively) when hovering in ground effect compared with control conditions. Such savings result largely from the substantial decreases in the induced velocity; however, the region of upwash beneath the bird's body for in ground effect hovering most likely augments these reductions. Because vegetational boundaries, either horizontal or otherwise, characterize many flowers visited by volant nectar-feeding insects as well as vertebrates, these energetic effects are likely to be general and suggest the need for further studies of wake–ground and wake–body interactions in ground effect hovering.

Acknowledgements. We thank Nir Sapir and Dennis Evangelista for their comments on the manuscript.

Funding statement. E.J.K. was supported by an NSF Integrative Graduate Education and Research Traineeship (IGERT) from UC Berkeley's Center for Interdisciplinary Biological Inspiration in Education and Research (CiBER), V.M.O.-J. was supported by a UC University of California MEXUS-CONACYT fellowship, and M.W. was supported by the Swedish Research Council. Animal care and experimental protocols were approved by the UC Berkeley Institutional Animal Care and Use Committee (IACUC).

References

1. Leishman JG. 2006 *Principles of helicopter aerodynamics*, 2nd edn. Cambridge, UK: Cambridge University Press.
2. Johnson W. 1980 *Helicopter theory*. New York, NY: Dover Press.
3. Norberg UM. 1990 *Vertebrate flight*. Berlin, Germany: Springer.
4. Rayner JMV. 1994 Aerodynamic corrections for the flight of birds and bats in wind tunnels. *J. Zool.* **234**, 537–563. (doi:10.1111/j.1469-7998.1994.tb04864.x)
5. Rayner JMV, Thomas ALR. 1991 On the vortex wake of an animal flying in a confined volume. *Phil. Trans. R. Soc. Lond. B* **33**, 107–117. (doi:10.1098/rstb.1991.0100)
6. Lighthill MJ. 1979 A simple fluid flow model of ground effect on hovering. *J. Fluid Mech.* **93**, 781–797. (doi:10.1017/S0022112 079002032)
7. Withers PC, Timko PL. 1977 The significance of ground effect to the aerodynamic cost of flight and energetics of the black skimmer (*Rhyncops nigra*). *J. Exp. Biol.* **70**, 13–26.
8. Finn J, Carlsson J, Kelly T, Davenport J. 2012 Avoidance of headwinds or exploitation of ground effect: why do birds fly low? *J. Field Ornithol.* **83**, 192–202. (doi:10.1111/j.1557-9263.2012.00369.x)
9. Rayner JMV. 1991 On the aerodynamics of animal flight in ground effect. *Phil. Trans. R. Soc. Lond. B* **334**, 119–128. (doi:10.1098/rstb.1991.0101)
10. Aldridge HDJN. 2009 Flight kinematics and energetics in the little brown bat, *Myoris lucifugus* (Chiroptera: Vespertilionidae), with reference to the influence of ground effect. *J. Zool.* **216**, 507–517. (doi:10.1111/j.1469-7998.1988.tb02447.x)
11. Park H, Choi H. 2010 Aerodynamic characteristics of flying fish in gliding flight. *J. Exp. Biol.* **213**, 3269–3279. (doi:10.1242/jeb.046052)
12. Blake RW. 1979 The energetics of hovering in the mandarin fish (*Synchropus picturatus*). *J. Exp. Biol.* **82**, 25–33.

13. Webb PW. 2002 Kinematics of plaice, *Pleuronectes platessa*, and cod, *Gadus morhua*, swimming near the bottom. *J. Exp. Biol.* **205**, 2125–2134.
14. Nowroozi BN, Strother JA, Horton JM, Summers AP, Brainerd EL. 2009 Whole-body lift and ground effect during pectoral fin locomotion in the northern spearnose poacher (*Agonopsis vulsa*). *Zoology* (*Jena*) **112**, 393–402. (doi:1016/j.zool.2008.10.005)
15. Light JS. 1993 Tip vortex geometry of a hovering helicopter rotor in ground effect. *J. Am. Helicopter Soc.* **38**, 34–42. (doi:10.4050/JAHS.38.34)
16. Pereira JCF, Maia N, Pereira JMC. 2009 A computational fluid dynamics study of a 2D airfoil in hovering flight under ground effect. *CMES-Comp. Model. Eng.* **49**, 113–141.
17. Gao T, Lu X. 2008 Insect normal hovering flight in ground effect. *Phys. Fluids* **20**, 087101. (doi:10.1063/1.2958318)
18. Chai P, Dudley R. 1995 Limits to vertebrate locomotor energetics suggested by hummingbirds hovering in heliox. *Nature* **377**, 722–725. (doi:10.1038/377722a0)
19. Chai P, Dudley R. 1996 Limits to flight energetics of hummingbirds hovering in hypodense and hypoxic gas mixtures. *J. Exp. Biol.* **199**, 2285–2295.
20. Ortega-Jiménez VM, Dudley R. 2012 Flying in the rain: hovering performance of Anna's hummingbirds under varied precipitation. *Proc. R. Soc. B* **279**, 3996–4002. (doi:10.1098/rspb.2012.1285)
21. Tobalske BW, Warrick DR, Clark CJ, Powers DR, Hedrick TL, Hyder GA, Biewener AA. 2007 Three-dimensional kinematics of hummingbird flight. *J. Exp. Biol.* **210**, 2368–2382. (doi:10.1242/jeb.005686)
22. Bartholomew GA, Lighton JR. 1986 Oxygen consumption during hover-feeding in free-ranging Anna's hummingbirds. *J. Exp. Biol.* **123**, 191–199.
23. Welch K. 2011 The power of feeder-mask respirometry as a method for examining hummingbird energetics. *Comp. Biochem. Physiol. A, Mol. Integr. Physiol.* **158**, 276–286. (doi:10.1016/j.cbpa.2010.07.014)
24. Suarez RK, Brown GS, Hochachka PW. 1986 Metabolic sources of energy for hummingbird flight. *Am. J. Physiol.* **251**, R537–R542.
25. Brobeck JR, Dubois AB. 1980 Energy exchange. In *Medical physiology*, vol. II (ed. VB Mountcastle), pp. 1351–1365. St Louis, MO: D. V. Mosby Co.
26. Ellington CP. 1984 The aerodynamics of hovering insect flight. VI. Lift and power requirements. *Phil. Trans. R. Soc. Lond. B* **305**, 145–181. (doi:10.1098/rstb.1984.0054)
27. Altshuler DL, Dudley R, Ellington CP. 2004 Aerodynamic forces of revolving hummingbird wings and wing models. *J. Zool.* **264**, 327–332. (doi:10.1017/S0952836904005813)
28. Morris CR, Nelson FE, Askew GN. 2010 The metabolic power requirements of flight and estimations of flight muscle efficiency in the cockatiel (*Nymphicus hollandicus*). *J. Exp. Biol.* **213**, 2789–2796. (doi:10.1242/jeb.035717)
29. Cheeseman IC, Bennett WE. 1955 *The effect of the ground on a helicopter rotor in forward flight*. Aeronautical Research Council reports and memoranda, no. 3021. London, UK: HMSO.
30. Hayden JS. 1976 *The effect of the ground on helicopter hovering power required*. Washington, DC: 32nd American Helicopter Society Forum.
31. Truong TV, Yoon KJ, Park HC, Kim MJ, Byun DY. 2013 Aerodynamic forces and flow structures of the leading edge vortex on a flapping wing considering ground effect. *Bioinspir. Biomim.* **8**, 036007. (doi:10.1088/1748-3182/8/3/036007)
32. Maeda M, Liu H. 2013 Ground effect in fruit fly hovering: a three-dimensional computational study. *J. Biomech. Sci. Eng.* **8**, 344–355. (doi:10.1299/jbse.8.344)
33. Rozhdestvensky KV. 2000 *Aerodynamics of a lifting system in extreme ground effect*, 1st edn. Berlin, Germany: Springer.
34. Altshuler DL, Princevac M, Pan H, Lozano J. 2009 Wake patterns of the wings and tail of hovering hummingbirds. *Exp. Fluids* **46**, 835–846. (doi:10.1007/s00348-008-0602-5)
35. Su J-Y, Ting S-C, Chang Y-H, Yang J-T. 2012 A passerine spreads its tail to facilitate a rapid recovery of its body posture during hovering. *J. R. Soc. Interface* **9**, 1674–1684. (doi:10.1098/rsif.2011.0737)
36. Nathan ND, Green RB. 2012 The flow around a model helicopter main rotor in ground effect. *Exp. Fluids* **52**, 151–166. (doi:10.1007/s00348-011-1212-1)
37. Fradenburgh EA. 1960 The helicopter and the ground effect machine. *J. Am. Helicopter Soc.* **5**, 26–28. (doi:10.4050/JAHS.5.24)
38. Warrick DR, Tobalske BW, Powers DL. 2005 Aerodynamics of the hovering hummingbird. *Nature* **435**, 1094–1097. (doi:10.1038/nature03647)
39. Pournazeri S, Segre PS, Princevac M, Altshuler DL. 2013 Hummingbirds generate bilateral vortex loops during hovering: evidence from flow visualization. *Exp. Fluids* **54**, 1439. (doi:10.1007/s00348-012-1439-5)
40. Wolf M, Ortega-Jimenez VM, Dudley R. 2013 Structure of the vortex wake in hovering Anna's hummingbirds (*Calypte anna*). *Proc. R. Soc. B* **280**, 20132391. (doi:10.1098/rspb.2013.2391)
41. Lima SL. 1991 Energy, predators, and the behaviour of feeding hummingbirds. *Evol. Ecol.* **5**, 220–230. (doi:10.1007/BF02214229)
42. Stiles FG. 1995 Behavioral, ecological and morphological correlates of foraging for arthropods, by the hummingbirds of a tropical wet forest. *Condor* **97**, 853–878. (doi:10.2307/1369527)
43. Dudley R. 2000 *The biomechanics of insect flight: form, function, evolution*. Princeton, NJ: Princeton University Press.